Conformation of a Heptadecapeptide Comprising the Segment Encephalitogenic in Rhesus Monkey†

William S. Price,‡ George L. Mendz,*,‡ and Russell E. Martenson§

Department of Biochemistry, The University of Sydney, NSW 2006, Australia, and Laboratory of Cerebral Metabolism, National Insitute of Mental Health, Bethesda, Maryland 20892

Received February 16, 1988; Revised Manuscript Received July 8, 1988

ABSTRACT: The 17-residue peptide FKLGGRDSRSGSPMARR derived from myelin basic protein, containing an epitope encephalitogenic in rhesus monkey, has been studied in aqueous solution by high-resolution one- and two-dimensional carbon and proton nuclear magnetic resonance spectroscopy. The resonances of the spectra from both nuclei were assigned with the aid of two-dimensional correlated spectroscopy, pH and solvent titrations, and one-dimensional spin-decoupling techniques and by comparison of the spectra of the heptadecapeptide with those of a phosphorylated form of the peptide, the pentadecapeptide FKLGGRDSRSGSPMA, and the nonapeptide FKLGGRDSR. Amide proton temperature coefficients, coupling constants, ^{13}C spin–lattice relaxation times, and nuclear Overhauser effect data suggest the existence of three structured regions comprising residues 3–6, 7–12, and 12–14 in the solution conformations of the encephalitogenic heptadecapeptide.

Chronic recurrent experimental autoimmune encephalomyelitis (EAE) in primates produces histopathological changes close to those observed in multiple sclerosis in man (Rauch & Roboz-Einstein, 1974; Wisniewski & Keith, 1977; Raine et al., 1978). An encephalitogenic determinant for rhesus monkey has been located in a 14-residue peptide FKLGGRDSRSGSP-hS isolated by peptic digestion and cyanogen bromide cleavage fromthe C-terminal end of myelin basic protein (MBP), where it comprises residues 152–165 (Karkhanis et al., 1975).

The MBP C-terminal heptadecapeptide comprising residues 152–168 contains the tetradecapeptide determinant and is itself encephalitogenic. There are similarities between amino acid sequences of the determinant causing EAE in guinea pig (Eylar et al., 1970), rabbit (Shapira et al., 1971), and rhesus monkey:

guinea pig

FSW GAE GQK

rabbit

THY GSL PQK

rhesus monkey

FKL GGR DSR SGSP-hS

The first two peptides contain an aromatic residue in the N-terminal region, a polar C-terminus with a long cationic side chain, and a central pair of residues (GA and GS) sterically favorable to the formation of reverse-turn conformations (Lewis et al., 1973). The first nine residues of the rhesus monkey determinant present similar features to the nonapeptides encephalitogenic in guinea pig and rabbit.

A cell-mediated reactivity to MBP and to the guinea pig determinant has been reported in tumor-bearing mice but not in controls (Yong & Halliday, 1982). The peptide comprising the first nine residues of the monkey encephalitogen shows similar reactivity in tumor-bearing mice (W. J. Halliday, personal communication). Nuclear magnetic resonance (NMR) studies of the guinea pig and rabbit encephalitogens in aqueous solutions suggested the presence of reverse turns at the GA and the GS pair of residues, respectively (Mendz et al., 1982; Mendz & Moore, 1983). Studies of the guinea pig determinant and of the nonapeptide N-terminal segment of the rhesus monkey determinant in DMSO suggested the existence of high statistical weight conformations with turns about the GA and GG pairs, respectively (Sadikot & Moore, 1983; Mendz et al., 1984). However, the nonapeptide segment FKLGGRDSR showed no activity in rhesus monkey (P. R. Carnegie, personal communication).

These observations suggest the recognition of different conformations by the rhesus monkey receptor site and by those of the guinea pig or rabbit. The investigation by ^{1}H and ^{13}C NMR spectroscopy of the conformation of the heptadecapeptide FKLGGRDSRSGSPMARR in aqueous solutions presented here finds its motivation in the closeness between the physiology of rhesus monkey and man and in the possible role of chronic relapsing EAE as a model for multiple sclerosis.

Materials and Methods

The preparation of the heptadecapeptide from rabbit MBP was performed as described by Martenson and co-workers (1981). A small amount (<20%) of the naturally occurring protein is phosphorylated at serine-163 corresponding to serine-12 in the peptide. A pure sample of the phosphorylated peptide was separated by chromatography on CM-cellulose (Martenson et al., 1983). The shorter pentadecapeptide, residues 152–166, was obtained by cleavage of the heptadecapeptide. Rabbit peptide 152–168 (52 mg) was incubated at 310 K for 2 h in 10 mL of 0.1 M NH_4HCO_3 (pH 8.2) containing 0.5 mg of carboxypeptidase B (Sigma, Type I) and 0.1 mg of soybean trypsin inhibitor (Sigma, Type I-S). The digest was lyophilized and then dissolved in several milliliters of 0.01 M HCl and subjected to gel filtration through a column (3.2 × 95 cm) of Sephadex G-25 fine to remove the enzyme. The single peptide peak was lyophilized and then dissolved in 0.01 M NH_4HCO_3 (pH 8.2) and applied to a column (2.5 × 17 cm) of Whatman CM-23 equilibrated with 0.01 M NH_4HCO_3 (278 K). The first peptide peak eluted (39 mg) with a 4-L gradient of 0.01–0.15 M buffer and was collected

† This work has been supported by grants from the National Health and Medical Research Council of Australia.

‡ The University of Sydney.

§ National Institute of Mental Health.

0006-2960/88/0427-8990$01.50/0

and identified as peptide 152–166 on the basis of tryptic peptide mapping (Martenson et al., 1983).

The nonapeptide FKLGGRDSR was synthesized by Peninsula Laboratories, San Carlos, CA. Analysis by high-performance liquid chromatography showed no detectable impurities. The peptide was used without further purification.

For NMR runs to observe nonexchangeable proton resonances the peptide was lyophilized in 99.75% ^2H_2O and then in 100% ^2H_2O. For measurements of the amide proton resonances, the peptide was lyophilized from H_2O and then dissolved in a 20/80 (v/v) mixture of $^2H_2O/H_2O$. Samples were prepared in 5-mm high-precision tubes for ^1H NMR experiments and in 10-mm precision tubes for ^{13}C runs. Peptide concentrations ranged between 2 and 20 mM for ^1H NMR experiments and between 20 and 75 mM for ^{13}C NMR experiments. The pH was adjusted with concentrated solutions of ^2HCl and NaO^2H and measured with an Activon 109 meter and a combined Ingold 6030-02 microelectrode. Quoted pH values are meter readings uncorrected for isotope effect. Immediately prior to measurements of the temperature dependence of the chemical shift of amide proton resonances, peptide solutions placed in NMR tubes were bubbled gently with ultrapure argon gas (CIG, Mascot, NSW, Australia) for 30 min and the tubes sealed quickly with septum caps.

Spectra were recorded with a Bruker WM-400 and a Varian XL-400 spectrometer operating in the Fourier transform mode with quadrature detection. All spectra were acquired at 298 K unless otherwise stated.

Typical acquisition parameters for one-dimensional (1D) proton spectra at 400 MHz were the following: spectral width, 4.8 kHz; pulse width, 8–16 μs; acquisition time, 1.7 s; average of 128 free induction decays. Amide proton resonances were observed by using the binomial (1 5 10 10 5 1) solvent suppression pulse sequence (Hore, 1983), which gives a broad region of near-zero excitation centered on the H_2O resonance. Spin-decoupling difference spectra were acquired by the procedures of Brown and Wüthrich (1981). Transient nuclear Overhauser enhancements (NOE) in the rotating frame were measured by the method of Bothner-by et al. (1984) with relaxation periods of 0.25 s. Steady-state NOE difference spectra were obtained with a frequency saturation time of 3.0 s by the method of Jones et al. (1978).

Two-dimensional (2D) homonuclear correlated spectroscopy (COSY) was used as an aid to proton spectral assignment. Spectra were acquired by using standard absolute-value and phase-sensitive double-quantum filtered COSY Bruker and Varian sequences. Spectra of 1024 × 1024 or 2048 × 2048 data points were obtained from 512 or 1024 individual experiments. The spectra are presented in absolute-value mode, with sine-bell apodization along t_1 and t_2. Accumulation of 48 free induction decays per experiment resulted in typical acquisition times of 14–25 h. Two-dimensional nuclear Overhauser enhancement spectroscopy (NOESY) and rotating-frame exchange spectroscopy (ROESY) were used to obtain information about peptide conformations. Standard Bruker and Varian sequences with mixing times ranging from 0.08 to 0.35 s were employed to obtain spectra of 1024 × 1024 data points from 512 individual experiments. The 2D spectra were symmetrized with standard programs and are presented in phase-sensitive mode.

One-dimensional ^{13}C spectra were acquired at 100.6 MHz with the following: spectral width, 20 kHz; pulse width, 20–30 μs; acquisition time of 0.8 s; relaxation delay, 2.5 s; average of 1024 free induction decays. Broadband Waltz decoupling was employed to decouple protons from the carbon nuclei.

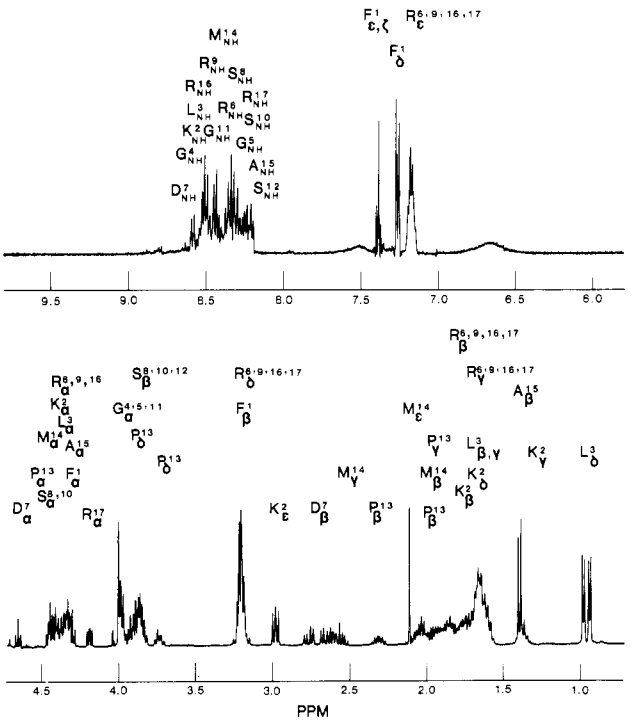

FIGURE 1: Proton NMR spectra of the heptadecapeptide FKLGGRDSRSGSPMARR at 298 K. The top spectrum shows the aromatic and amide regions of the peptide in H_2O solution at pH 2.28. The bottom spectrum shows the aliphatic region in ^2H_2O solution at pH 6.00.

Spectra are presented after a line broadening of 3 Hz by exponential multiplication. Spin–lattice relaxation times were measured by using the inversion-recovery pulse sequence with a relaxation delay of 5 s (Vold et al., 1968).

Two-dimensional heteronuclear shift-correlated spectroscopy experiments were performed with standard Varian pulse sequences. This allowed the ^{13}C resonances of protonated carbons to be assigned from the ^1H assignments. There are 2048 data points per scan, and 256 experiments were transformed with no window functions.

RESULTS

(1) Assignment of Proton Resonances. The aliphatic region of the 1D spectrum of the heptadecapeptide in ^2H_2O at 298 K and pH 6.00 and the aromatic and amide regions in H_2O and pH 2.28 are shown in Figure 1. The aliphatic region of the phase-sensitive double-quantum filtered COSY spectrum in ^2H_2O at 298 K and pH 2.28 is shown in Figure 2. Resonances were assigned by examining the correlations in the COSY contour map, by spin-decoupling techniques, by pH titrations, and by comparisons with the spectra of the phosphorylated heptadecapeptide, the pentadecapeptide, and the nonapeptide and also with literature values for other peptides. Table I summarizes the assignments of the proton resonances.

The 17-residue peptide is composed of 10 different types of amino acids. There are two levels of assignments to be established: first, residue types, and then individual residues. The correlations in the COSY spectrum allow unequivocal assignment of certain spin systems. The correlation patterns for Ala, Arg, Leu, Lys, and Pro residues are unambiguous. Since the peptide contains no Glu or Gln, the spin system of Met was also unambiguously assigned. Thus, 9 of the 17 residues can be assigned to definite types on the basis of the 2D homonuclear correlated map. Spin-decoupling difference spectra lead to precise chemical shift values for the resonances concerned.

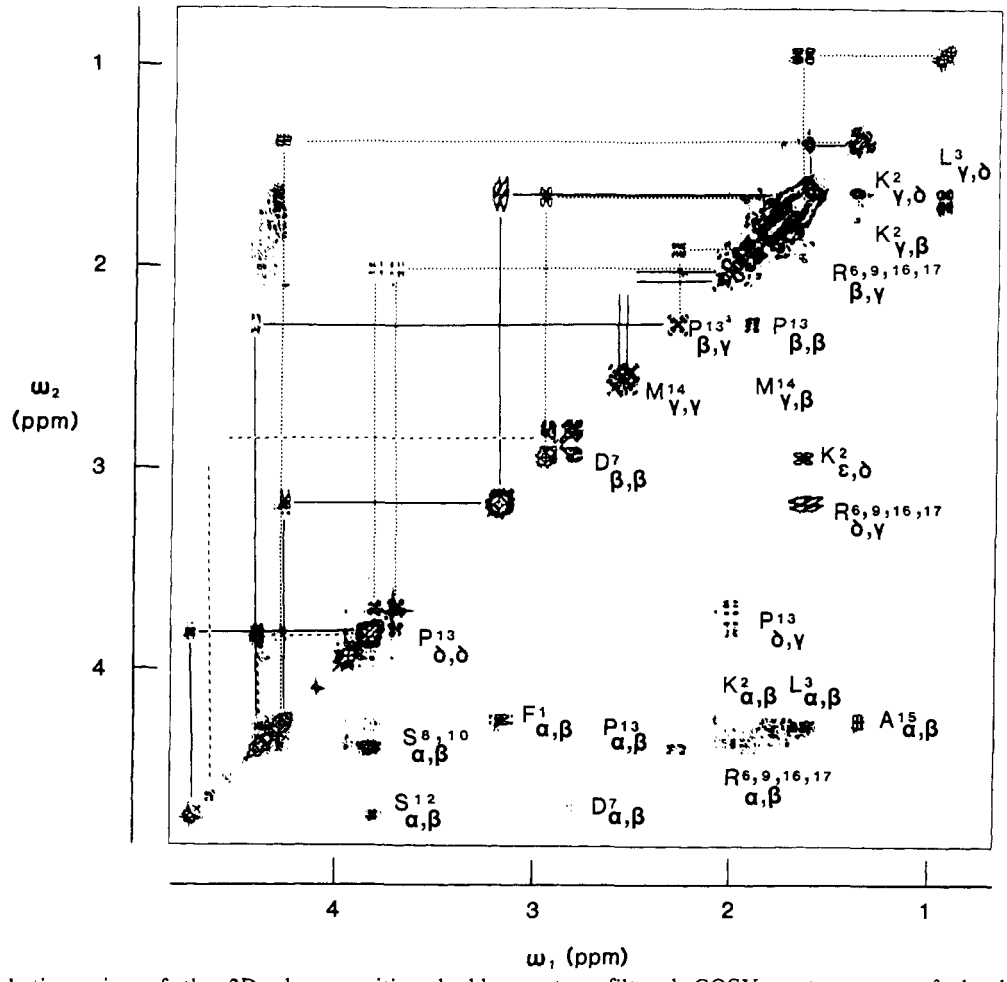

FIGURE 2: Aliphatic region of the 2D phase-sensitive double-quantum filtered COSY contour map of the heptadecapeptide FKLGGRDSRSGSPMARR in ^2H_2O solution at 298 K and pH 2.28.

The remaining types of residues are Phe, Ser, Asp, and Gly. The first three types have ABX/BM spin systems in ^2H_2O solutions and are easily identified. The β-CH_2 protons appear as characteristic 2 × 4 line resonances in the 1D spectrum of the peptide. In the 2D COSY contour plot they show connectivities only to α-methine peaks. The methylene resonances of Asp were distinguished by their marked upfield shift from 2.835 and 2.969 to 2.659 and 2.767 ppm when the pH was changed from 2.28 to 6.0. At pH 2.28 the Ser-β-CH_2 lines are found between 3.846 and 3.884 ppm. The Phe-β-CH_2 resonances occur at 3.198 and 3.220 at pH 2.28. These values are comparable with those observed for small peptides (Bundi & Wüthrich, 1979). The glycine resonances were identified by comparing the 1D and 2D COSY spectra and noting that these peaks do not have connectivities to any other resonance.

A COSY contour plot of the peptide in H_2O solution allowed the assignment of the amide proton resonances of Lys-2, Asp-7, Ser-12, Ala-15, and the three Gly. Spectral overlap in both the amide proton and the α-proton regions of the spectrum precluded any further assignments from this correlated map. The rest of the couplings between α-proton and amide proton peaks were found by irradiating the α-CH resonances in sequential spin-decoupling difference experiments performed in H_2O solutions of the peptide.

Resonances were assigned to specific residues after the assignments to residue types were made. Since there is only one of each Phe-1, Lys-2, Leu-3, Asp-7, Pro-13, Met-14, and Ala-15, the corresponding peaks were completely assigned. The types of residues occurring more than once in the sequence are three Gly, four Arg, and three Ser. Assignment of these

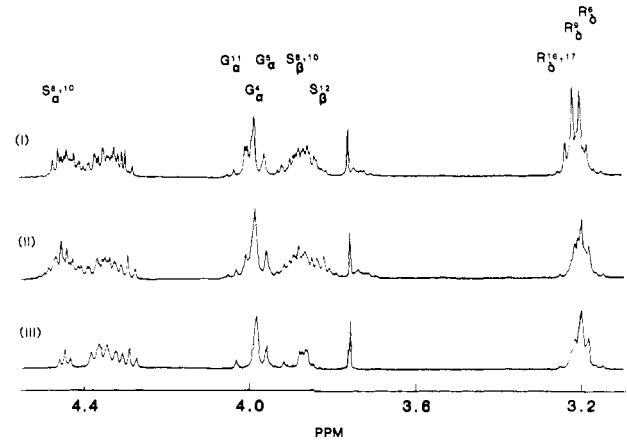

FIGURE 3: Comparison of part of the aliphatic region of the spectra of the heptadecapeptide (I), pentadecapeptide (II), and nonapeptide (III) in ^2H_2O solutions at 298 K and pH 2.28.

resonances to specific residues was made by comparing spectra of the heptadeca-, pentadeca-, and nonapeptides.

(*i*) *Glycine.* The glycine amide proton peak without a counterpart in the spectrum of the nonapeptide was assigned to Gly-11. The amide resonances of Gly-4 and Gly-5 had been assigned in the spectrum of the nine-residue peptide in DMSO solutions (Mendz et al., 1984). A solvent titration from DMSO to H_2O served to obtain the spectral positions of these peaks in aqueous solutions, and these assignments led to the ones for the α-proton resonances (Table I). The values were in good agreement with those measured by comparing the

Table I: ^{1}H Chemical Shifts of Resonances, $^3J_{NH-\alpha-CH}$ Coupling Constants, and Torsional Angles (ϕ) at 298 K and pH 2.28

residue	proton	δ	$^3J_{NH-\alpha-CH}$ (Hz)	$\phi^a \pm 4$ (deg)
Phe-1	α-CH	4.302		
	β-CH_2	3.198, 3.220		
	δ_1-, δ_2-CH	7.263		
	ϵ_1-, ϵ_2-CH	7.385		
	ζ-CH	7.403		
Lys-2	α-NH	8.509	7.2	−86, −154
	α-CH	4.360		
	β-CH_2	1.710, 1.770		
	γ-CH_2	1.396, 1.396		
	δ-CH_2	1.610, 1.672		
	ϵ-CH_2	2.973, 2.973		
Leu-3	α-NH	8.449	7.2	−86, −154
	α-CH	4.342		
	β-CH_2	1.653, 1.672		
	γ-CH	1.679, 1.679		
	δ_1-, δ_2-CH_3	0.943, 0.983		
Gly-4	α-NH	8.518	5.6	42, 78, −70, −170
	α-CH_2	3.983, 3.983		
Gly-5	α-NH	8.300	6.0	60, −75, −165
	α-CH_2	3.944, 4.002		
Arg-6	α-NH	8.342	6.4	−78, −162
	α-CH	4.320		
	β-CH_2	1.78, 1.85		
	γ-CH_2	1.671, 1.686		
	δ-CH_2	3.200, 3.200		
	ϵ-NH	7.176		
Asp-7	α-NH	8.588	7.6	−91, −149
	α-CH	4.655		
	β-CH_2	2.835, 2.969		
Ser-8	α-NH	8.316	6.4	−78, −162
	α-CH	4.444		
	β-CH_2	3.847, 3.881		
Arg-9	α-NH	8.381	7.2	−86, −154
	α-CH	4.400		
	β-CH_2	1.77, 1.82		
	γ-CH_2	1.648, 1.648		
	δ-CH_2	3.208, 3.208		
	ϵ-NH	7.716		
Ser-10	α-NH	8.262	6.8	−82, −158
	α-CH	4.438		
	β-CH_2	3.848, 3.881		
Gly-11	α-NH	8.419	6.0	60, −75, −165
	α-CH_2	3.991, 4.013		
Ser-12	α-NH	8.221	7.6	−91, −149
	α-CH	4.785		
	β-CH_2	3.840, 3.872		
Pro-13	α-CH	4.463		
	β-CH_2	1.938, 2.301		
	γ-CH_2	2.030, 2.030		
	δ-CH_2	3.734, 3.847		
Met-14	α-NH	8.359	6.8	−82, −158
	α-CH	4.420		
	β-CH_2	1.955, 2.074		
	γ-CH_2	2.572, 2.616		
	ϵ-CH_3	2.112, 2.112		
Ala-15	α-NH	8.225	5.6	42, 78, −70, −170
	α-CH	4.310		
	β-CH_3	1.395		
Arg-16	α-NH	8.446	7.2	−86, −154
	α-CH	4.332		
	β-CH_2	1.70, 1.76		
	γ-CH_2	1.671, 1.686		
	δ-CH_2	3.218, 3.218		
	ϵ-NH	7.176		
Arg-17	α-NH	8.277	6.8	−82, −158
	α-CH	4.377		
	β-CH_2	1.69, 1.78		
	γ-CH_2	1.671, 1.686		
	δ-CH_2	3.218, 3.218		
	ϵ-NH	7.176		

[a] The torsional angles ϕ were calculated by using the parameters A = 5.0, B = 1.5, and C = 2.5 Hz (De Marco & Llinas, 1980). These parameters were taken as exact values. An error of ±15° is obtained for the values of the torsional angles when the calculations include an error of 0.8 Hz for A, B, and C.

spectra of the nona-, pentadeca-, and heptadecapeptides (Figure 3). The methylene protons of Gly form an AB spin system in ^2H_2O solutions. Accurate chemical shifts were determined for these two-spin systems by using values of the coupling constants measured directly from the spectrum (Jackman & Sternhell, 1969).

(*ii*) *Arginine.* At pH 2.28 the Arg-α-CH lines of residues 6, 9, 16, and 17 have chemical shifts between 4.320 and 4.400 ppm. The amide proton resonances corresponding to these residues have chemical shifts of 8.277, 8.342, 8.381, and 8.446 ppm. Arg-6-α-NH is found at 8.340 ppm in the spectrum of the nonapeptide. The peak with chemical shift 8.342 ppm was assigned to Arg-6 in the spectrum of the heptadecapeptide by comparison. The chemical shift of the corresponding resonance in the pentadecapeptide is found at 8.339 ppm; the other arginine amide proton peak in the spectrum of this peptide, at 8.385 ppm, was then assigned to the arginine residue in position 9. The Arg-9-α-NH proton in the heptadecapeptide spectrum was assigned to the resonance at 8.381 ppm by comparison. The two arginine amide proton peaks left to be assigned in the spectrum of the heptadecapeptide correspond to Arg-16 and Arg-17. Changing the pH of the solution from 2.27 to 3.5 produced a shift of 0.135 ppm in an arginine α-methine resonance. The shift was attributed to the effect of the deprotonation of the end carboxyl group of the peptide. Consequently, this resonance was assigned to Arg-17. The increase in pH induced shifts of 0.148 and 0.038 ppm on the amide resonances at 8.227 and 8.446 ppm, respectively. From these data, the peak at 8.227 ppm was assigned to the amide proton of Arg-17 and the one at 8.446 ppm to that of Arg-16. The assignment of Arg-17-α-NH was confirmed with the observation that this resonance is coupled to the peak previously assigned to Arg-17-α-CH. The chemical shifts thus derived for the spin systems of the four arginine residues are in agreement with those obtained for the δ-CH_2 resonances by direct comparison of the spectra of the spectra of the three peptides (Figure 3).

(*iii*) *Serine.* There are three serine residues in the heptadecapeptide occurring at positions 8, 10, and 12. In the 2D correlated contour plot (Figure 2) cross-peaks between serine methine and methylene resonances indicated that there is one α-CH peak at 4.785 ppm, close to the residual water resonance. The α-CH spectral lines of the other two serine residues occur at 4.438 and 4.444 ppm. The phosphorylated heptadecapeptide was employed to determine the resonances corresponding to Ser-12. The phosphate group attached to this residue causes deshielding of its protons, thereby shifting the resonances downfield (Figure 4). Two groups of lines observable only in the spectrum of the phosphorylated peptide have chemical shifts of 4.897 and 4.131 ppm. Selective irradiation showed that they are coupled; hence, they were assigned to the α-CH and β-CH_2 protons of Ser-12, respectively. In the spectrum on the nonphosphorylated peptide the corresponding chemical shifts are 4.785 for the methine proton and 3.840 and 3.872 ppm for the methylene protons. The peak at 4.444 ppm was assigned to the Ser-8-α-CH proton by comparison with the spectrum of the nonapeptide in which the corresponding resonance has the same chemical shift. The third serine spin system, comprising peaks at 4.438, 3.848, and 3.881 ppm, is thus that of Ser-10. Figure 3 shows the α-CH and β-CH_2 spectral regions of the serine residues in the nona-, pentadeca-, and heptadecapeptides. The chemical shifts of the Ser-β-CH_2 protons were obtained by analysis of the AB spin system resulting from decoupling the methine protons. The values of the coupling constants of each of the three Ser-β-CH_2 were

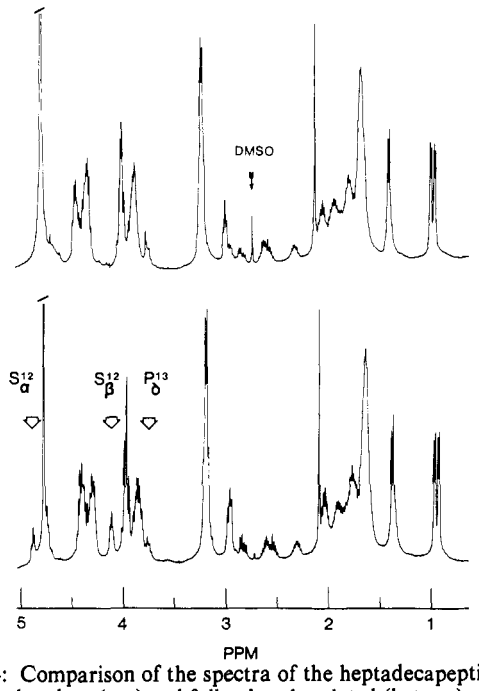

FIGURE 4: Comparison of the spectra of the heptadecapeptide with naturally abundant (top) and fully phosphorylated (bottom) serine-12 at 298 K and pH 3.0.

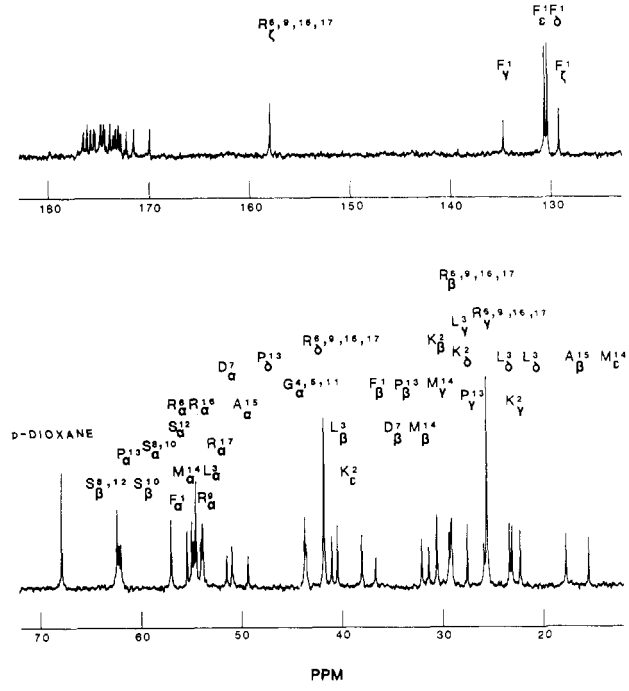

FIGURE 5: One-dimensional ^{13}C spectrum of the heptadecapeptide FKLGGRDSRSGSPMARR in $^{2}H_2O$ solution at 300 K and pH 2.45.

measured from the spin-decoupled difference spectra.

(2) Assignment of ^{13}C Resonances. Figure 5 shows a 1D ^{13}C spectrum of the heptadecapeptide; assignments and chemical shifts are summarized in Table II. The heteronuclear shift-correlated 2D contour plot shown in Figure 6 led to assignments of most protonated ^{13}C peaks in the spectrum. The chemical shifts obtained are in good agreement with literature values (Grathwohl & Wüthrich, 1974). The overlap of resonances in the α-CH region of the proton and carbon spectra did not allow umambiguous assignment of the peaks corresponding to lysine and leucine residues from the 2D ^{13}C–^{1}H correlations. Moreover, the similarity of ^{1}H chemical shifts observed between the methine resonances of two serine

Table II: ^{13}C Chemical Shifts of Resonances, Spin–Lattice Relaxation Times (NT_1), and Nuclear Overhauser Enhancements (NOE) for Proton-Bearing Carbon Nuclei[a]

residue	carbon	δ	$NT_1 \pm 6\%$ (ms)	NOE	τ_{int} (ns)
Phe-1	α-CH	55.48	402	1.87	0.108
	β-CH_2	38.19	494	2.43	0.084
	δ_1-, δ_2-CH	130.32	490	1.71	0.077
	ϵ_1-, ϵ_2-CH	130.59	477	2.15	0.076
	ζ-CH	129.18	333	1.41	0.181
Lys-2	α-CH	54.55	301	2.19	0.263
	β-CH_2	30.73	636	2.35	0.047
	γ-CH_2	23.23	774	3.00	0.036
	δ-CH_2	27.70	1004	2.89	0.026
	ϵ-CH_2	40.57	1448	3.00	0.016
Leu-3	α-CH	53.91	329	2.17	0.186
	β-CH_2	41.14	524	2.44	0.065
	γ-CH	27.70	502	2.89	0.070
	ζ_1-CH_3	22.43	2079	2.63	0.011
	ζ_2-CH_3	23.50	1665	2.64	0.014
Gly-4,5,11	α-CH_2	43.78	346	2.01	0.160
	α-CH_2	43.64	346	1.76	0.160
Arg-6	α-CH	54.95	276	2.10	0.424
	β-CH_2	29.30	396	2.00	0.112
	γ-CH_2	25.72	614	2.42	0.050
	δ-CH_2	41.89	652	2.57	0.046
Asp-7	α-CH	51.55	269	2.10	0.514
	β-CH_2	36.79	342	1.86	0.165
Ser-8	α-CH	57.01	302	2.02	0.259
	β-CH_2	62.36	416	2.46	0.100
Arg-9	α-CH	54.06	310	1.92	0.232
	β-CH_2	29.30	396	2.00	0.112
	γ-CH_2	25.72	614	2.42	0.050
	δ-CH_2	41.89	652	2.57	0.046
Ser-10	α-CH	57.01	302	2.02	0.259
	β-CH_2	62.00	430	2.49	0.094
Ser-12	α-CH	54.95	276	2.10	0.424
	β-CH_2	62.36	416	2.46	0.100
Pro-13	α-CH	62.17	238	1.87	
	β-CH_2	32.22	408	2.52	0.105
	γ-CH_2	26.45	672	2.38	0.043
	δ-CH_2	49.43	360	1.73	0.142
Met-14	α-CH	54.76	274	1.93	0.446
	β-CH_2	31.53	398	2.89	0.111
	γ-CH_2	30.73	636	2.35	0.047
	ϵ-CH_3	15.62	8700	1.73	0.002
Ala-15	α-CH	50.98	334	2.83	0.178
	β-CH_3	17.88	1326	2.15	0.182
Arg-16	α-CH	54.55	301	2.19	0.263
	β-CH_2	29.30	396	2.00	0.112
	γ-CH_2	25.72	614	2.42	0.050
	δ-CH_2	41.89	652	2.57	0.046
Arg-17	α-CH	53.82	324	2.17	0.197
	β-CH_2	29.47	396	2.00	0.112
	γ-CH_2	25.72	614	2.42	0.050
	δ-CH_2	41.89	652	2.57	0.046

[a] Rotational correlation times for internal motion (τ_{int}) were calculated by assuming isotropic overall motion of the peptide chain with $\tau_{mol} = 0.27$ ns.

residues (4.438 and 4.444 ppm) and between those of arginine residues precluded direct assignment of the corresponding ^{13}C spectral lines to specific residues through the correlated map.

The methods employed to complete the spectral assignment of the heptadecapeptide were pH titrations and comparison with the ^{13}C spectra of the nona- and pentadecapeptides. The ^{13}C spectrum of the nonapeptide in aqueous solution was assigned from the ^{1}H spectrum by means of a 2D heteronuclear shift-correlated map. The chemical shifts of the α-CH resonances (with the exception of Ser-8 and Arg-9) are in good agreement with those of putative peaks in the spectra of the pentadeca- and heptadecapeptides. The Lys-2, Leu-3, and Arg-6-α-CH resonances were then assigned by comparison.

Results of pH titrations of the nona- and heptadecapeptides are shown in Figure 7. The pH titration of the nonapeptide

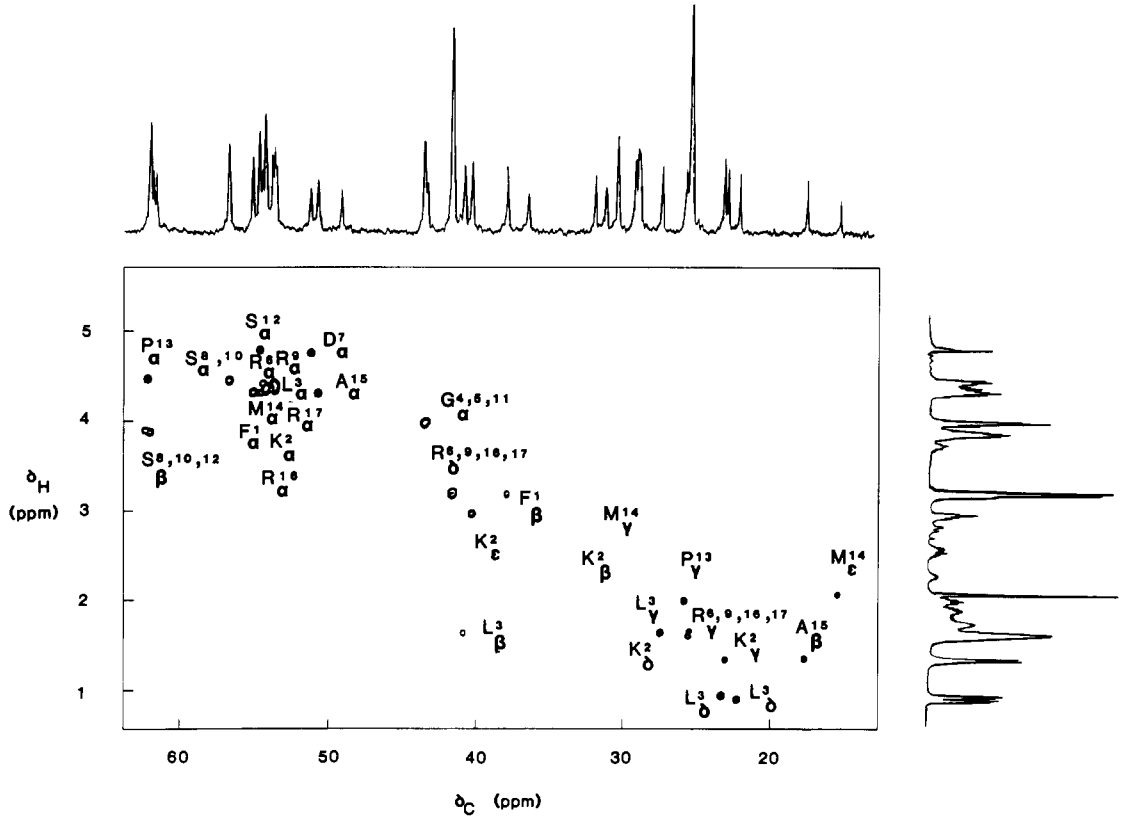

FIGURE 6: Aliphatic region of the 2D heteronuclear ^{13}C–^{1}H shift-correlated map of the heptadecapeptide FKLGGRDSRSGSPMARR in $^{2}H_2O$ at 300 K and pH 2.45.

confirmed the Arg-α assignments. Since Arg-9 is at the carboxyl terminus, the chemical shift of its α-CH resonance, 53.82 ppm at pH 2.04 and 56.20 ppm at pH 10.25, is more susceptible to pH. Two of the three remaining unassigned Arg-α-CH resonances in the heptadecapeptide are not found in the spectrum of the pentadecapeptide. One of these exhibited a large chemical shift variation with pH, 53.82 ppm at pH 2.28 to 56.03 ppm at pH 8.00, and was consequently assigned to Arg-17-α; the other one was assigned to Arg-16-α. The remaining unassigned Arg-α-CH peak is that of Arg-9 by elimination.

The pH titrations of the 9- and 17-residue peptides allowed confirmation of the Phe-1-α resonance with a pH-induced chemical shift change of 1.12 ppm from pH 5.45 to 9.0 in both peptides. This observation is consistent with the effects that arise from ionization of the N-terminal amino group. Ser-12-α-CH exhibited a characteristic change in chemical shift between pH 2.45 and 4.75 (Figure 7). Among the Ser-β-CH_2 resonances, only one shifted in this pH range and was therefore assigned to Ser-12-β. The resonances corresponding to Ser-8 in the spectrum of the heptadecapeptide were assigned by comparison with the spectrum of the shorter peptide. The remaining unassigned α-CH and β-CH_2 serine resonances are those of Ser-10.

(*3*) *Amide Proton Temperature Coefficients.* The temperature dependence of the chemical shifts of the amide proton resonances were analyzed by linear least-squares regression analysis giving the $-d\delta/dT$ values in Table III. As a control of the $d\delta/dT$ of the amide protons, the δ of the α-CH protons were found to be practically independent of temperature (Higashima et al., 1979).

(*4*) *Spin–Lattice Relaxation Times and Heteronuclear Overhauser Effect Values for* ^{13}C *Nuclei.* Measurements of longitudinal relaxation times and of heteronuclear Overhauser effects were performed with peptides obtained from three

Table III: Temperature Coefficients of Amide Proton Resonances of the Three Peptides at pH 2.28

	$-d\delta/dT$ (ppb/K)		
	nona-peptide	penta-decapeptide	hepta-decapeptide
Phe-1			
Lys-2	6.297	6.235	6.236
Leu-3	8.351	8.233	8.120
Gly-4	8.007	8.074	8.057
Gly-5	5.778	5.818	5.758
Arg-6	6.561	6.368	6.757
Asp-7	6.741	6.546	6.592
Ser-8	5.514	5.887	5.962
Arg-9	5.705	5.823	5.640
Ser-10		5.869	5.765
Gly-11		5.930	6.264
Ser-12		5.427	5.678
Pro-13			
Met-14		7.968	7.591
Ala-15		7.968	7.364
Arg-16			7.987
Arg-17			8.008

different preparations of the heptadecapeptide. Under similar experimental conditions the NT_1 and NOE values for the protonated ^{13}C nuclei in the peptide were the same within experimental error and are recorded in Table II. Measured NOE values indicate that observed longitudinal relaxation times are determined solely by the dipolar mechanism (Doddrell et al., 1972). At pH 2.45 the α-CH resonances of Ser-12 and Arg-6 and those of Arg-16 and Lys-2 overlap; the observed spin–lattice relaxation times for each pair were 0.276 and 0.301 s, respectively. Owing to the spectral overlap, these values could not be assigned unambiguously to any of the peaks. At pH 4.1 all four peaks are resolved. Measured longitudinal relaxation times at this pH gave values of 0.281 s for Ser-12-α-CH, 0.329 s for Arg-6-α-CH, 0.326 s for Lys-2-α-CH,

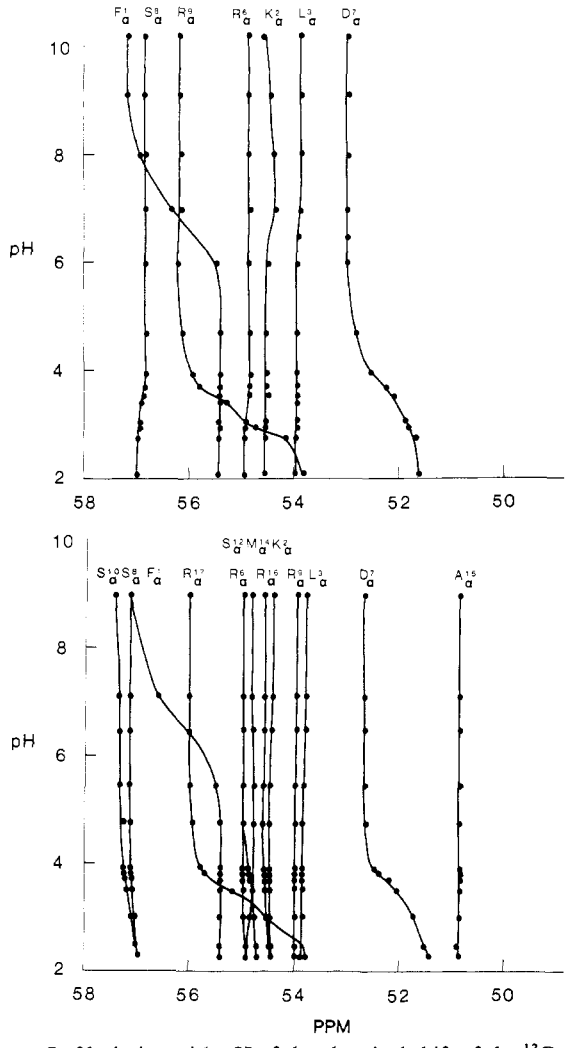

FIGURE 7: Variation with pH of the chemical shift of the ^{13}C resonances of the nonapeptide (top) and of the heptadecapeptide (bottom). Spectra were acquired at 300 K.

and 0.302 s for Arg-16-α-CH. The data from the measurements at both pH were in agreement within experimental error, with the exception of the values for Arg-17-α-CH. The discrepancy can be explained by the different protonation state of the end carboxyl group at each pH. Consequently, it was reasonable to assume that Ser-12-α has an NT_1 value which is at most 0.276 s.

The NT_1 data provided information regarding relative mobilities of different regions of the peptide backbone and side chains. Application of the expression for a rigid rotor (Doddrell et al., 1972) to the relaxation time of Pro-13-α-CH of 0.238 s yielded an upper limit correlation time for the overall isotropic motion of the peptide chain, τ_{mol}, of 0.27 ns, based on a C–H bond length of 109 pm. Backbone and side-chain NT_1 values were analyzed by the method of Wallach (1967) and Levine (1974) giving correlation times, τ_{int}, for rotations about carbon–carbon bonds (Table II). Although the absolute values of τ_{int} are dependent on the approximation made in the dynamic model, the values calculated for different positions along the backbone or along the side chains provided information concerning relative mobilities. The τ_{int} values indicate two regions of restricted mobility: between Asp-7 and Ser-10 and from Ser-12 to Met-14.

(*5*) *Coupling Constants.* The $^3J_{\alpha\text{-NH}-\alpha\text{-CH}}$ coupling constants are listed in Table I along with the corresponding torsional angles ϕ. The torsional angles were calculated by using the Karplus relations and the measured ^3J values. The parameters used are based on data from ferrichromes in aqueous solutions; the solid-state structure of these rigid peptides is believed not to alter on solution in water (De Marco & Llinas, 1980). The ϕ values for the MBP peptide, however, are likely to be weighted averages of a number of conformations.

(*6*) *Nuclear Overhauser Effects.* Homonuclear NOE data are particularly useful for conformational studies, since the dipolar interaction is strongly dependent on internuclear distance. In general, it is possible to observe the effect of dipole–dipole interactions between a pair of protons that are within about 500 pm of each other (Kumar et al., 1981). An Overhauser effect between protons on nonadjacent residues provides information of a compact conformation of high statistical weight. The NOE effects detected by either 1D or 2D techniques were small, even between protons located in the same residue. The relatively small size of the peptide and the apparent short correlation times measured suggest that the observable NOE at 400 MHz will be restricted to small values. In addition to intraresidue NOE and effects between nearest neighbors, a few long-range dipolar interactions were observed in peptide solutions at neutral pH (Figure 8). These were between Gly-4-α-CH_2 and Lys-ϵ-CH_2, Arg-δ-CH_2 and Ser-β-CH_2, Asp-α-CH and Pro-α-CH, Asp-α-CH and Phe-δ-CH_2, and Arg-17-α-CH and Phe-β-CH_2.

Discussion

Evidence for the existence of high statistical weight conformations of the heptadecapeptide in solution was provided by long-range NOE effects, by the amide proton temperature coefficients, and by the longitudinal relaxation times of the backbone carbon nuclei. The temperature coefficient data indicate that the amide protons of Gly-5, Ser-8, Arg-9, Ser-10, and Ser-12 are moderately shielded from solvent, those of Leu-3, Gly-4, Met-14, Ala-15, Arg-16, and Arg-17 are fully exposed to solvent, and the rest have a medium exposure. Turns and loops in a polypeptide chain result in different degrees of exposure to solvent of amide protons. In flexible linear peptides, the spin–lattice relaxation times of backbone carbon nuclei are usually very similar, except for those of the nuclei at the ends of the chain, which have notably larger mobilities. Restriction of motion of backbone carbon nuclei is observed in the regions Asp-7–Ser-10 and Ser-13–Met-14. There is also some degree of constraint in the motion of the methine carbons of Lys-2 and Leu-3.

The NOE between protons of nonadjacent residues can be explained only by nonextended structures for the peptide. The small magnitude of the Overhauser effects detected in both the rotating frame and the laboratory frame suggests that the peptide molecule is very flexible. Consequently, it is unlikely that all close interproton distances in the peptide have yielded observable NOE at 400 MHz; nevertheless, those that have been measured provide constraints in the delineation of permissible structures. Phe-1, Lys-2, Asp-7, and Pro-13 are unique residues in the primary structure, and the long-range effects in which nuclei located at these residues are involved determine the broad outlines of putative high statistical weight solution conformations of the peptide. On the other hand, the overlap of the α-CH_2 resonances of glycine residues, of the δ-CH_2 resonances of arginine residues 6 and 9, and of the β-CH_2 resonances of the three serine residues introduces a certain ambiguity in the interpretation of the NOE results. Assuming the simplest cases in which residues are not subject to impossible steric constraints, the NOE data are interpreted as manifesting interactions between the side chain of Lys-2 and the methylene protons of Gly-4 and between the side chains of Arg-9 and Ser-10.

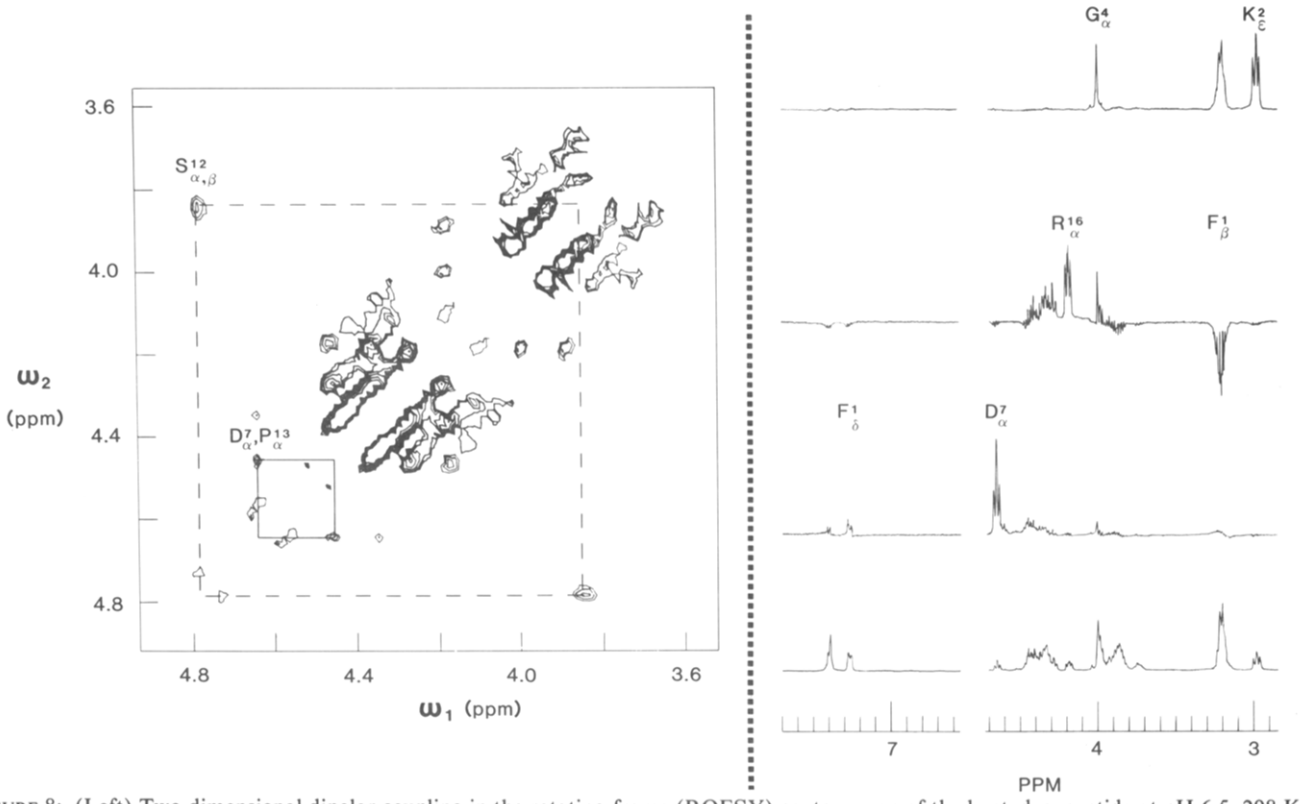

FIGURE 8: (Left) Two-dimensional dipolar coupling in the rotating-frame (ROESY) contour map of the heptadecapeptide at pH 6.5, 298 K, and 15 mM. Only the negative contours are presented. The intraresidue NOE of Ser-12 is presented as a reference. (Right) Steady-state NOE difference spectra representing long-range dipolar interactions. The bottom spectrum corresponds to the standard spectrum of the heptadecapeptide. The line irradiated in each case was Asp-7-α-CH, Arg-17-α-CH, and Lys-2-ϵ-CH_2. The NOE effect was observed on Phe-1-δ-CH_2, Phe-1-β-CH_2, and Gly-4-α-CH_2 resonances, respectively. Other peaks that appear in the difference spectra arise from incomplete subtraction.

The overall picture of the heptadecapeptide derived from the NMR data is that of a flexible molecule undergoing rapid tumbling in solution. There is also evidence supporting the existence of high statistical weight peptide conformations with structured regions, that is, conformations with sufficiently large populations and sufficiently long lifetimes that permitted the observation of dipolar interactions between different parts of the molecule and yielded average nonrandom values of specific NMR parameters. It is possible to construct a model that takes into account and is consistent with all the experimental data, but which does not constitute a unique interpretation of them. The main features of this model are three structured regions. This interpretation of the results does not require that the suggested structures in each region have similar statistical weights or that they be present simultaneously in a given molecule. Figure 9 shows schematically the backbone of a model in which, for reasons of brevity, the suggested structures for the three regions have been represented simultaneously. It should be noted that several interatomic distances are presented unrealistically short to provide visual emphasis to some features and that physical limitations of setting the model free-standing result in the backbone being portrayed in a quasi-planar fashion that is unlikely to correspond to any high statistical weight solution conformation.

In the first region Phe-1 would come into proximity to Asp-7 with the aromatic ring located "above" a loop formed by the backbone of residues 1–6 and moving in a region where the loop provides some degree of isolation from the solvent. This structure would have a turn of the backbone at Lys-2 and Leu-3, resulting in some constraint in the motion of the carbon nucleus of the former. The differences between the relaxation times of the α-carbons in this segment of the peptide were small; however, the difference of 45 ms between the measured

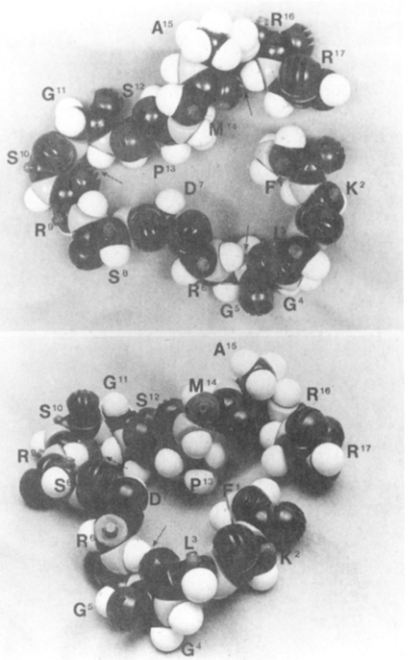

FIGURE 9: (Top) Schematic model of a backbone conformation of high statistical weight consistent with the data for the peptide. The arrows indicate the position of possible CO···HN hydrogen bonds. (Bottom) Same model rotated 70° about a horizontal axis on the plane of the paper. The side chains of Gly-4, Gly-5, Gly-11, Pro-13, and Ala-15 are included.

T_1 for Leu-2 and for Gly-4 was significant beyond experimental error (Table II). When the motion of these nuclei was analyzed by examining the corresponding internal correlations, the difference was about 60% (Table II). Calculated τ_{int} take

into consideration the overall peptide motion and the fact that the α-carbons of leucine residues are methines and those of glycine residues are methylenes. The side chains of both residues would be able to move freely in the solvent. That of Lys-2 would be oriented away from the space defined by the loop and directed "forward" in a manner that allows a dipolar interaction with the methylene protons of Gly-4. The side chain of Leu-3 would be oriented toward that of Phe-1 and above it, providing further isolation from solvent to the aromatic moiety. The loop would be completed by a tighter turn at Gly-4 and Gly-5. Of the sterically possible ϕ torsional angles calculated from the measured coupling constants for Leu-3, Gly-4, Gly-5, and Arg-6, the set of average values (−154, −86, 60, −162) is close to the values corresponding to type-II β-turn structures obtained as the result of minimum-energy calculations carried out on protected pentapeptides (Lewis et al., 1973). The correspondence is particularly close for the values (−155, −87, 52, −158) obtained from computations on *N*-acetyl *N'*-methyl Ala-Ala-Ala-Ala amide. A type-II β-turn comprising residues 3–6 would leave the amide proton of Gly-4 exposed to the solvent and that of Gly-5 oriented toward the inner space of the loop, shielding it from the solvent, in agreement with the data for temperature coefficients. The presence of a hydrogen bond between residues i and $i + 3$ (in the present instance Leu-3 and Arg-6, respectively) is not a necessary condition for the formation of tight turns. Statistical analyses of X-ray crystallography data of proteins showed that $i - (i + 3)$ hydrogen bonds in loops were longer and had less favorable geometries than hydrogen bonds in α-helices or β-sheets (Baker & Hubbard, 1984). An explanation for this observation was that the out-of-plane angles measured in $i - (i + 3)$ hydrogen bonds clustered about 60°. Assuming an approximately sp^2-hybrid carbonyl oxygen atom with the lone pairs in the plane of the peptide bond, the hydrogen atom would then not be well directed toward the lone pair orbital. These hydrogen bonds presumably contribute to stabilize the bend structure, but about half of the turns quoted by Chou and Fasman (1977) do not appear to have such a hydrogen bond.

There are no absolute thresholds of amide proton resonance temperature coefficient values below which hydrogen bonding of a NH proton is unequivocal (Smith & Pease, 1980), and moderate to high values have been obtained for temperature coefficients of amide protons involved in intramolecular hydrogen bonding in aqueous solutions: e.g., −5.5 ppb/K for the NH resonance of Gly-4 in the tetrapeptide VPGG (Urry & Ohnishi, 1974), −7.3 and −7.99 ppb/K for the amide proton resonance of Val-4 for the monomeric and polymeric forms, respectively, of the repeat peptide of elastin (Urry & Long, 1976), −5.3 ppb/K for the NH resonance of Gly-3 in an analogue of a repeat hexapeptide of tropoelastin (Khaled et al., 1979). Hence, the temperature coefficient measured for the heptadecapeptide did not rule out the possibility that a significant mole fraction of the amide proton of Arg-6 may be involved in intramolecular bonding. If this proton were involved in a hydrogen bond with the carbonyl group of Leu-3, it would usually have a low temperature coefficient. But if the orientation of the bond places the proton partially outside the loop, as depicted in the model, the temperature coefficient would indicate only a medium degree of protection from the solvent, as it was experimentally observed. The methine carbon of Arg-6 located at the end of the turn would be restricted in its motion but with the side chain able to move freely in the solvent.

A second major structure would be another loop bringing Asp-7 into proximity with Pro-13, making possible the observed dipolar interaction between the methine protons of both residues. The NMR data are consistent with this structure being less mobile than the one described above, with a turn about Ser-10 and Gly-11. This second loop would also define an "inner space" into which the amide protons of Ser-8, Arg-9, and Ser-10 would be oriented, in agreement with the temperature coefficient data for these protons. The long arginyl side chain would be oriented into the solvent and able to interact with the side chain of Ser-10. The spin–lattice relaxation time of the methine carbon of Ser-8 indicated that rotations about the ϕ torsional angle are not completely free in this residue. The value of the average ^3J coupling constant of its amide proton provided additional support of the existence of the structured region. Considering that among the calculated ϕ torsional angles for Arg-9, Ser-10, Gly-11, and Ser-12 the set of average values (−154, −82, 60, −149) is sufficiently close to the values corresponding to type-II β-turn, it is possible to interpret the experimental data in terms of such a bend in the segment Arg-Ser-Gly-Ser. Although (−60, 80), are the values for the ϕ torsional angles in the $i + 1$ and $i + 2$ positions calculated with optimal hydrogen bond between the $i + 3$ and i positions (Nemethy & Scheraga, 1980), the average values (−82, 60) obtained for Ser-10 and Gly-11 are in very good agreement with those observed in type-II β-turn protein chain reversals; for instance, the values of the ϕ torsional angles in residues 20–21 in egg white lysozyme determined by X-ray diffraction are (−90, 50) (Lewis et al., 1973). The spin–lattice relaxation times of the methine carbons of these residues can be interpreted also in terms of a β-turn. The measured value for the Gly-11 methylene carbon, corresponding to an internal correlation time of 0.16 ns, indicated unhindered motion, whereas the smaller relaxation time of the methine carbon of Ser-12, which yielded a correlation time of 0.424 ns (Table II), indicated a restriction in motion. The amide temperature coefficients of these two residues indicated a medium degree of protection for the Gly-11 proton and a more effective shielding for the proton of Ser-12. For reasons similar to those discussed above, the temperature coefficient of this amide proton did not rule out the existence of a hydrogen bond with the carbonyl oxygen of Arg-9. If this proton were involved in a hydrogen bond, the orientation of this bond, as depicted in the model, would place it within the space enclosed by the loop. The loop would be completed by the turn in the backbone imposed by the proline side chain. The strong downfield shift of the Ser-12-α-CH resonance can be explained by magnetic shielding of the proton by the pyrrolidone ring.

The segment comprised by the final four residues, Met-Ala-Arg-Arg, also appeared to have some structure. The spin–lattice relaxation time of the Met-14-α-CH carbon indicated restricted motion. The average value of the ^3J coupling constant of the alanyl suggested nonaverage random motion about the ϕ torsional angle, but the internal correlation time of its methine carbon had a value characteristic of unrestricted motion. Of the possible average values for the ϕ torsional angles for Ala-15 and Arg-16, the set (42, −154) is in very close agreement with the values (50, −145) calculated with optimal hydrogen bond for a type-I β-turn (Nemethy & Scheraga, 1980). However, the temperature coefficients of the amide protons of these four residues indicated full exposure to the solvent. Both sets of observations can be reconciled by bearing in mind that a hydrogen bond found at the end of the backbone, between the amide proton of Arg-17 and the carbonyl group of Met-14, would not be protected from solvent.

An alternative explanation is that the observed restrictions in motion simply arise from steric constraints posed by the bulky Met and Arg side chains. Finally, the NOE observed between Arg-17-α-CH and Phe-1-β-CH_2 suggested that this segment of the peptide is "bent" over the N-terminal region of the molecule.

The segments of the peptide that appear more structured are the sequences Leu-Gly-Gly-Arg, Asp-Ser-Arg-Ser-Gly-Ser, and Ser-Pro-Met. In the model we have described, the first segment is found at the end of the first loop. The backbone shows normal mobility in the first three residues and low mobility at Arg-6, with all side chains facing the solvent with the exception of that of Gly-5. The segment including residues 7–12 comprises the second loop and shows low backbone mobility, and the side chains are facing the solvent. In the third segment the backbone shows low mobility, but the proline ring faces at least partially into the inner space of the second loop and there may be steric constraints between the side chains of Met-14 and the two arginyls at the C terminus. From these considerations we suggest that the antigenic region is located in the segment comprising residues 7–12, which fulfills necessary conditions of mobility to fit into receptor sites and of exposure of side chains for recognition. Cleavage at residue 9 would destroy antigenic activity as it is observed with the nonapeptide. On the other hand, the peptide comprising residues 1–14 is fully active. Cleavage at residue 14 would keep the region between Asp-7 and Ser-12 intact, and activity would be preserved, since there appear not to be interactions with the four last residues of the heptadecapeptide. If the antigenic region were located at residues 12–14, it is reasonable to expect that a cleavage which would leave Met-14, in the form of homoserine-14, as the C-terminal residue of the peptide would affect antigenicity, but this is not the case. A final consideration that suggests segment 7–12 as the best candidate for the epitope is the presence, at physiological pH, of two charged residues, a positively charged arginyl and a negatively charged aspartyl.

ACKNOWLEDGMENTS

We are thankful to Dr. B. E. Chapman for help with the pulse sequences and to W. G. Lowe for technical assistance.

Registry No. FKLGGRDSRSGSPMARR, 38580-75-5.

REFERENCES

Baker, E. N., & Hubbard, R. E. (1984) *Prog. Biophys. Mol. Biol. 44*, 97–179.

Bothner-by, A. A., Stephens, R. L., Ju-mee Lee, Warren, C. D., & Jeanloz, R. W. (1984) *J. Am. Chem. Soc. 106*, 811–813.

Brown, L. R., & Wüthrich, K. (1981) *Biochim. Biophys. Acta 647*, 95–111.

Bundi, A., & Wüthrich, K. (1979) *Biopolymers 18*, 285–297.

Chou, P. Y., & Fasman, G. D. (1977) *J. Mol. Biol. 155*, 135–175.

De Marco, A., & Llinas, M. (1980) *J. Magn. Reson. 39*, 253–262.

Doddrell, D., Glushko, V., & Allerhand, A. (1972) *J. Chem. Phys. 56*, 3683–3689.

Eylar, E. H., Caccam, J., Jackson, J. J., Westall, F. C., & Robinson, A. B. (1970) *Science (Washington, D.C.) 168*, 1220–1223.

Grathwohl, C., & Wüthrich, K. (1974) *J. Magn. Reson. 13*, 217–225.

Higashima, T., Kobayashi, J., Nagai, V., & Miyazawa, T. (1979) *Eur. J. Biochem. 97*, 43–57.

Hore, P. J. (1983) *J. Magn. Reson. 55*, 283–300.

Jackman, L. M., & Sternhell, S. (1969) *Nuclear Magnetic Resonance Spectroscopy in Organic Chemistry*, pp 129–130, Pergamon, Oxford, U.K.

Jones, C. R., Sikakana, C. T., Hehir, S., Kiro, M.-C., & Gibbons, W. A. (1978) *Biophys. J. 24*, 815–832.

Karkhanis, Y. D., Carlo, D. J., Brostoff, S. W., & Eylar, E. H. (1975) *J. Biol. Chem. 250*, 1718–1722.

Khaled, MD. Abu, Sugano, H., & Urry, D. W. (1979) *Biochim. Biophys. Acta 577*, 273–284.

Kopple, K. D., Ohnishi, M., & Go, A. (1969) *J. Am. Chem. Soc. 91*, 4264–4272.

Kumar, A., Wagner, G., Ernst, R. R., & Wüthrich, K. (1981) *J. Am. Chem. Soc. 103*, 3654–3658.

Levine, Y. K., Birdsall, N. J. M., Lee, A. G., Metcalfe, J. C., Partington, P., & Roberts, G. C. K. (1974) *J. Chem. Phys. 60*, 2890–2899.

Lewis, P. N., Momany, F. A., & Scheraga, M. A. (1973) *Biochim. Biophys. Acta 303*, 211–229.

Martenson, R. E., Lüthy, V., & Deibler, G. E. (1981) *J. Neurochem. 36*, 58–68.

Martenson, R. E., Law, M. J., & Deibler, G. E. (1983) *J. Biol. Chem. 258*, 930–937.

Mendz, G. L., & Moore, W. J. (1983) *Biochim. Biophys. Acta 748*, 176–183.

Mendz, G. L., Moore, W. J., & Carnegie, P. R. (1982) *Aust. J. Chem. 35*, 1979–2006.

Mendz, G. L., Moore, W. J., King, G., & Wright, P. E. (1984) *Int. J. Pept. Protein Res. 24*, 208–217.

Nemethy, G., & Scheraga, H. A. (1980) *Biochem. Biophys. Res. Commun. 95*, 320–327.

Raine, C. S., Traugott, V., & Stone, S. H. (1978) *Science (Washington, D.C.) 201*, 445–448.

Rauch, H. C., & Roboz-Einstein, R. (1974) *J. Neurol. Sci. 23*, 99–116.

Sadikot, H., & Moore, W. J. (1983) *Aust. J. Chem. 36*, 33–41.

Shapira, R., McKneally, S., Chou, F. C., & Kibler, R. F. (1971) *Science (Washington, D.C.) 173*, 736–738.

Smith, J. A., & Pease, L. G. (1980) *CRC Crit. Rev. Biochem. 8*, 315–387.

Urry, D. W., & Ohnishi, T. (1974) *Biopolymers 13*, 1223–1234.

Urry, D. W., & Long, M. M. (1976) *CRC Crit. Rev. Biochem. 4*, 1–45.

Vold, R. L., Waugh, J. S., Klein, M. P., & Phelps, D. E. (1968) *J. Chem. Phys. 48*, 3831–3832.

Wallach, D. (1967) *J. Chem. Phys. 47*, 5258–5268.

Wisniewski, H. M., & Keith, A. B. (1977) *Ann. Neurol. 1*, 144–148.

Yong, W. K., & Halliday, W. J. (1982) *Br. J. Cancer 45*, 754–761.